Title

Differential Subsampling with Cartesian Ordering–MRA for Classifying Residual Treated Aneurysms

Journal

American Journal of Neuroradiology, 43(6)

ISSN

0195-6108

Authors

Shahrouki, P
Gupta, R
Belani, P
et al.

Publication Date

2022-06-01

DOI

10.3174/ajnr.a7532

Peer reviewed

Differential Subsampling with Cartesian Ordering–MRA for Classifying Residual Treated Aneurysms

P. Shahrouki, R. Gupta, P. Belani, A. Chien, A.H. Doshi, R. De Leacy, J.T. Fifi, J. Mocco, and K. Nael

ABSTRACT

BACKGROUND AND PURPOSE: Differential Subsampling with Cartesian Ordering (DISCO), an ultrafast high-spatial-resolution head MRA, has been introduced. We aimed to determine the diagnostic performance of DISCO-MRA in grading residual aneurysm in comparison with TOF-MRA in patients with treated intracranial aneurysms.

MATERIALS AND METHODS: Patients with endovascular treatment and having undergone DISCO-MRA, TOF-MRA, and DSA were included for review. The voxel size and acquisition time were 0.75 × 0.75 × 1 mm^3/6 seconds for DISCO-MRA and 0.6 × 0.6 × 1 mm^3/6 minutes for TOF-MRA. Residual aneurysms were determined using the Modified Raymond-Roy Classification on TOF-MRA and DISCO-MRA by 2 neuroradiologists independently and were compared against DSA as the reference standard. Statistical analysis was performed using the κ statistic and the χ^2 test.

RESULTS: Sixty-eight treated intracranial aneurysms were included. The intermodality agreement was $\kappa =$ 0.82 (95% CI, 0.67–0.97) between DISCO and DSA and 0.44 (95% CI, 0.28–0.61) between TOF and DSA. Modified Raymond-Roy Classification scores matched DSA scores in 60/68 cases (88%; $\chi^2 = 144.4$, $P < .001$ for DISCO and 46/68 cases (68%; $\chi^2 = 65.0$, $P < .001$) for TOF. The diagnostic accuracy for the detection of aneurysm remnants was higher for DISCO (0.96; 95% CI, 0.88–0.99) than for TOF (0.79; 95% CI, 0.68–0.88).

CONCLUSIONS: In patients with endovascularly treated intracranial aneurysms, DISCO-MRA provides superior diagnostic performance in comparison with TOF-MRA in delineating residual aneurysms in a fraction of the time.

ABBREVIATIONS: ARC = Autocalibrating Reconstruction for Cartesian; CE = contrast-enhanced; DISCO = Differential Subsampling with Cartesian Ordering; EVT = endovascular treatment; IA = intracranial aneurysm; IQR = interquartile range; MRRC = Modified Raymond-Roy Classification; NPV = negative predictive value; PPV = positive predictive value

Endovascular treatment (EVT) is considered the primary strategy for intracranial aneurysms (IAs) in most cases in many institutions, with lower morbidity and mortality compared with microsurgical clipping for most aneurysms.[1,2]

However, subtotal occlusion or recanalization has been raised as a limitation of EVT, with reports of up to 20% of patients demonstrating deterioration in occlusion status on follow-up imaging.[3-5] Therefore, noninvasive imaging such as CTA or MRA is commonly used in the serial follow-up of these patients, and while there is no universally accepted strategy, the frequency and type of imaging used should be balanced against patient safety and cost.[6]

For institutions that use MRA for follow-up of patients with treated aneurysms, both TOF-MRA and contrast-enhanced MRA (CE-MRA) can be used, each with some benefits and drawbacks. During the past 2 decades, there has been an increasing evolution of CE-MRA techniques, with improved diagnostic performance, which was achieved, at least partly, via the introduction of fast imaging tools such as Generalized Autocalibrating Partially Parallel Acquisition or Autocalibrating Reconstruction for Cartesian (ARC) imaging and a variety of *k*-space undersampling schemes.[7-11]

An ultrafast, high-spatiotemporal-resolution CE-MRA, using Differential Subsampling with Cartesian Ordering (DISCO) has been introduced for the depiction of IAs.[12] In this study, we aimed to assess the diagnostic accuracy of DISCO-MRA in treated aneurysms and to classify aneurysm occlusion in a comparative analysis with TOF-MRA, with DSA as the reference standard.

Received September 11, 2021; accepted after revision April 14, 2022.

From the Department of Radiological Sciences (P.S., A.C., K.N.), University of California Los Angeles, Los Angeles, California; and Departments of Radiology (R.G., P.B., A.H.D., K.N.) and Neurosurgery (R.D.L., J.T.F., J.M.), Icahn School of Medicine at the Mount Sinai Hospital, New York, New York.

This work was supported by the National Institutes of Health (NIH R01HL152270) for Aichi Chien.

Please address correspondence to Kambiz Nael, MD, Department of Radiological Sciences, University of California Los Angeles, 757 Westwood Plaza, Suite 1621, Los Angeles, CA 90095–7532; e-mail: kambiznael@gmail.com; @KambizNael

Indicates open access to non-subscribers at www.ajnr.org

Indicates article with online supplemental data.

http://dx.doi.org/10.3174/ajnr.A7532

MATERIALS AND METHODS

Patients

This retrospective review of prospectively collected data was approved by the Mount Sinai Hospital Institutional Review Board. Patients with IAs who presented between January 2016 and January 2019 were reviewed and included if they had an aneurysm treated by EVT and had follow-up DSA and MRA after treatment.

Image Acquisition

CE-MRA and TOF-MRA were concurrently performed in all patients on a 3T MR imaging system (Discovery MR750; GE Healthcare) using an 8-channel head coil for signal reception.

For CE-MRA, a single-echo 3D radiofrequency-spoiled gradient-echo sequence was used with the following parameters: TR/TE = 3.7/1.4 ms; flip angle = 12°; matrix = 320 × 256 mm^2; FOV = 240 × 192 mm^2; 160 slices × 1.0 mm thick. The DISCO *k*-space segmentation scheme using pseudorandom variable-density *k*-space segmentation and a view-sharing reconstruction was applied,[12] in addition to ARC with an acceleration factor of 2 in both phase-encoding and section-encoding directions. With these settings, a 3D volume with voxel sizes of 0.75 × 0.75 × 1 mm^3 was obtained covering the entire head in a 6-second acquisition. A timing bolus was used to determine the contrast transit time to the intracranial carotid bifurcation during a 30- second image acquisition. A total of 0.05 mmol/kg of gadolinium was injected at 1.5 mL/s to perform CE-MRA.

Multislab TOF-MRA was performed with 6 axial slabs of 32 slices per slab, each 1 mm thick with the following parameters: TR/TE = 20/5.7 ms; flip angle = 20°; matrix = 320 × 296 mm^2; FOV = 180 × 180 mm^2; and ARC × 2 (phase-encoding), resulting in the acquisition of 3D voxel sizes of 0.6 × 0.6 × 1 mm^3 during a 6-minute acquisition time.

DSA was performed via transfemoral access and by selective catheterization of the ICA and/or the vertebral artery as appropriate and according to the aneurysm location. Images were obtained in the anteroposterior and lateral projections and in 2 oblique projections (−45° and +45°) for each catheterization. We used the following parameters: matrix = 1024 × 1024 mm; FOV = 17 cm, resulting in spatial resolution of 0.15 × 0.15 mm. The injected volume of contrast medium ranged between 3 and 5 mL per injection. Additional 3D rotational projections were obtained for challenging cases and based on the interventionist's judgment at the time of the procedure in 17 patients (25%).

Image Analysis

The aneurysm occlusion status was evaluated using the Modified Raymond-Roy Classification (MRRC): class I = complete obliteration; II = residual neck; IIIa = contrast opacification within the coil interstices of a residual aneurysm; or IIIb = contrast opacification outside the coil interstices along the residual aneurysm wall.[13]

Image analysis was performed independently by 2 board-certified neuroradiologists (K.N. and P.B. with 10 and 6 years of experience, respectively) who were blinded to DSA results. DISCO-MRAs and TOF-MRAs were analyzed in different reviewing sessions, and the studies were introduced in a random order to minimize recall bias. All-source MRA data were available and reviewed on a commercially available 3D workstation (Vitrea software, Version 7.14; Vital Images) with 3D multiplanar reformations available. Disagreements in the grading of residual aneurysms were resolved by a consensus read, which was, in turn, used for comparative analysis against DSA. The aneurysm occlusion class on DSA was extracted from our aneurysm data registry, which is prospectively collected and updated as patients undergo treatment.

Table 1: Patient and aneurysm characteristics

Characteristics	
Female (No.) (%)	59 (86)
Age (mean) (yr)	59.4 (SD, 11.4)
Aneurysm location	
Internal carotid artery (No.) (%)	28 (41)
Anterior cerebral artery (No.) (%)	3 (4)
Anterior communicating artery (No.) (%)	8 (12)
Middle cerebral artery (No.) (%)	4 (6)
Posterior communicating artery (No.) (%)	17 (25)
Posterior circulation[a] (No.) (%)	8 (12)
Endovascular treatment	
Stent only (No.) (%)	6 (9)
Coil only (No.) (%)	34 (50)
Stent-assisted coil (No.) (%)	28 (41)

[a] Includes aneurysms involving the posterior cerebral artery ($n = 1$), vertebral artery ($n = 3$), and basilar artery ($n = 4$).

Statistical Analysis

Continuous data were presented as means with SDs or median with interquartile range (IQR), and categoric data were presented as absolute values with percentages. κ statistic and 95% confidence intervals were calculated to determine both the interobserver and intermodality agreement. The χ^2 test was used to determine differences in MRRC matches between DISCO-MRA and TOF-MRA. The sensitivity, specificity, positive predictive value (PPV), negative predictive value (NPV), and accuracy of DISCO and TOF-MRA for the detection of aneurysm remnants were determined. Statistical analysis was performed on SPSS software (Version 27.0; IBM). A P value $< .05$ was considered statistically significant.

RESULTS

Sixty-eight treated IAs in 68 patients (59 women; mean age, 59.4 [SD, 11.4] years) were included for analysis (Table 1). Aneurysm locations included the anterior circulation (60/68, 88%) and posterior circulation (8/68, 12%; Table 1). The median time between the MRA and DSA was 99 days (IQR = 29–186 days), with DSA performed before MRA in most cases (47/68, 69%). The median time between endovascular treatment to the first follow-up examination (MRA or DSA) was 598 days (IQR, 567–622 days).

The interobserver agreement for the MRRC of aneurysms was near-identical for DISCO-MRA and TOF-MRA ($\kappa = 0.61$; 95% CI, 0.45–0.77 for DISCO-MRA and $\kappa = 0.63$; 95% CI, 0.44–0.81 for TOF-MRA). The intermodality agreement for the MRRC was higher between DISCO and DSA ($\kappa = 0.82$; 95% CI, 0.67–0.97) than between TOF and DSA ($\kappa = 0.44$; 95% CI, 0.28–0.61).

Analysis of the MRRC revealed a higher number of class matches between the DISCO and DSA evaluations (60/68, 88%; $\chi^2 = 144.4$, $P < .001$) compared with TOF and DSA (46/68, 68%; $\chi^2 = 65.0$, $P < .001$) (Table 2).

Among 33 completely occluded treated aneurysms (MRRC I), 32 (97%) were correctly identified by both DISCO and TOF-MRA.

Table 2: MRRC class matches between DSA and DISCO-MRA and TOF-MRA[a]

	DISCO-MRA					TOF-MRA				
DSA	I	II	IIIa	IIIb	Total	I	II	IIIa	IIIb	Total
I	32	1	0	0	33 (49)	32	1	0	0	33 (49)
II	2	15	3	0	20 (29)	11	9	0	0	20 (29)
IIIA	0	2	6	0	8 (12)	1	4	3	0	8 (12)
IIIB	0	0	0	7	7 (10)	1	4	0	2	7 (10)
Total	34 (50)	18 (26)	9 (13)	7 (10)	68 (100)	45 (66)	18 (26)	3 (4)	2 (3)	68 (100)

[a] Data are presented as counts with percentages in parenthesis.

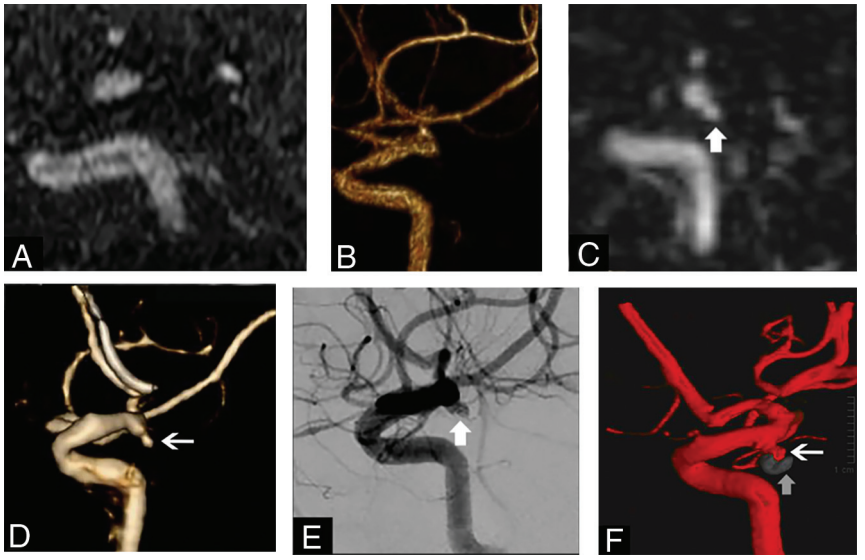

FIG 1. A 56-year-old woman status post coil embolization of a posterior communicating artery aneurysm. Sagittal multiplanar reformats and volume-rendered images from TOF-MRA (*A* and *B*) and DISCO-MRA (*C* and *D*) in addition to sagittal projection and 3D from DSA (*white arrows in E* and *F*) are shown. There is a recanalized aneurysm measuring approximately 5 mm (MRRC IIIB) seen on the DSA images (*E* and *F*). Note the location of the embolization coil mass (*vertical arrow* on *F*). The recanalized aneurysm is visualized with a similar size and conspicuity on DISCO-MRA (*arrows* on *C* and *D*), while it is not clearly seen on TOF-MRA (*A* and *B*).

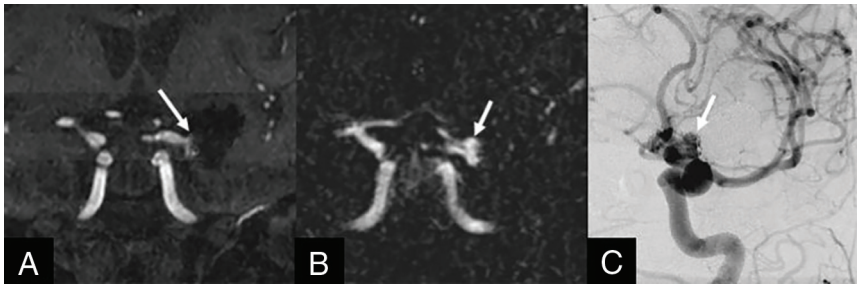

FIG 2. A 70-year-old woman status post endovascular treatment of a left ICA bifurcation aneurysm. Coronal multiplanar reformats from TOF-MRA (*A*) and DISCO-MRA (*B*) and coronal-oblique DSA (*C*) are shown. There is a 6-mm residual neck (MRRC II) at the base of the coil embolization mass on DSA (*arrow* in *C*), which is also noted with a similar size and conspicuity on DISCO-MRA (*arrow* in *B*). The residual aneurysm neck is less conspicuous on TOF-MRA (*arrow* in *A*), where it was scored as MRRC I by 1 observer.

However, class matches for recanalized IAS (MRRC II–IV) against DSA were 28/35 (80%) for DISCO-MRA and 14/35 (40%) for TOF-MRA (Table 2). In particular, among patients with higher grade remnants (MRRC IIIa/IIIb, $n = 15$), 13 (86%) remnants were correctly identified on DISCO-MRA, while only 5 (33%) were identified on TOF-MRA. Examples of aneurysm recanalization seen on TOF-MRA and DISCO-MRA in comparison with DSA are shown in Figs 1 and 2.

The diagnostic accuracy of DISCO-MRA was higher than that of TOF-MRA for the detection of aneurysm remnants (MRRC II–IIIb; Online Supplemental Data). The specificity and PPV were comparable between the modalities (equal low false-positive counts), with the sensitivity and NPV of DISCO-MRA being higher than that of TOF-MRA (Online Supplemental Data).

In a subgroup analysis comparing aneurysms that were treated with stents versus no stents, similar results were identified, with the specificity and PPV being comparable, while the sensitivity and NPV were substantially higher in DISCO-MRA versus TOF-MRA (Online Supplemental Data). Figure 3 shows an example of an aneurysm treated by a stent; the higher grade of the aneurysm remnant was correctly identified by DISCO-MRA.

The sensitivity and NPV in patients treated with stents were 100% and 100%, respectively, for DISCO-MRA in comparison with 63% and 74% for TOF-MRA. In the stented subgroup, a total of 13 aneurysm remnants were misclassified by TOF-MRA versus 3 by DISCO-MRA. The breakdown of aneurysm-remnant misclassification in this group for TOF-MRA versus DISCO-MRA was the following: grade I (1 versus 1), grade II (5 versus 0), grade IIIa (4 versus 2), and grade IIIb (3 versus 0).

In the absence of stent placement, the sensitivity and NPV were 89% and 88% for DISCO in comparison with 63% and 68% for TOF-MRA (Online Supplemental Data). In the nonstented subgroup, a total of 9 aneurysm remnants were misclassified by TOF-MRA versus 5 misclassified by DISCO-MRA. The breakdown of aneurysm-remnant misclassification in this group for TOF-MRA versus DISCO-MRA was the following: grade II (6 versus 5), grade IIIa (1 versus 0), and grade IIIb (2 versus 0).

DISCUSSION

Results showed that in patients with IAs treated by EVT, ultrafast, high-spatial-resolution CE-MRA achieved by DISCO outperformed TOF-MRA compared with the conventional standard for the evaluation of residual aneurysms. DISCO-MRA had higher

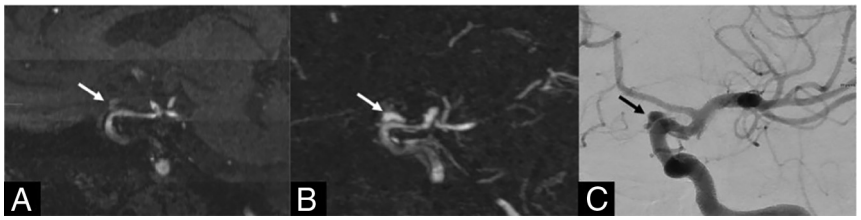

FIG 3. A 67-year-old woman with an aneurysm of the left supraclinoid ICA, treated with a Pipeline Embolization Device (Medtronic) stent. Sagittal oblique multiplanar reformats from TOF-MRA (*A*) and DISCO-MRA (*B*) and sagittal-oblique DSA (*C*) are shown. There is a 4-mm residual aneurysm (MRRC IIIb) projecting superior to the stent on DSA (*arrow* in *C*), which is also noted with similar size and conspicuity on DISCO-MRA (*arrow* in *B*). The residual aneurysm is less conspicuous on TOF-MRA (*arrow* in *A*), where it was scored as MRRC I by one observer and II by the other.

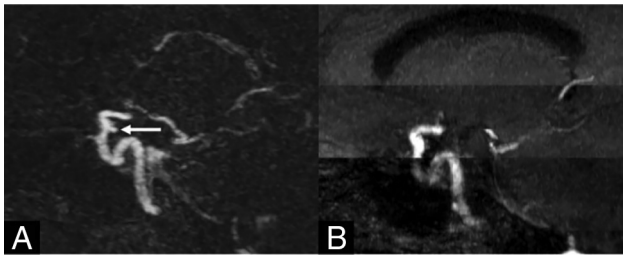

FIG 4. A 57-year-old woman with an aneurysm of the right supraclinoid ICA, treated with coil embolization. Sagittal oblique multiplanar reformats from DISCO-MRA (*A*) and TOF-MRA (*B*) are shown. There is a 3-mm posteriorly projecting residual aneurysm at the base of coil embolization noted on DISCO-MRA (*arrow* in *A*), which was acquired during a 6-second acquisition time. Note that the residual aneurysm is not well-evaluated on the concurrent motion-degraded TOF-MRA, which was obtained during an approximately 6-minute acquisition time.

accuracy and agreement with DSA than TOF-MRA and was performed in a fraction of the time.

The specificity and PPV were similar between DISCO and TOF-MRA (>90%), and the sensitivity and NPV were markedly lower for TOF-MRA for the detection of aneurysm remnants. When there was no remnant (MRRC I), both DISCO and TOF-MRA correctly identified the MRRC in most cases (97% for both). We showed that the difference in class matches was most pronounced for the higher classes, particularly class III. The MRRC highlights the importance of differentiating between class IIIa and IIIb because the latter has a higher risk of incomplete occlusion, recanalization, and possibly rupture.[13,14] Therefore, underestimating class III aneurysms, as was more common with TOF-MRA in our study (10 for TOF-MRA compared with 2 for DISCO-MRA) could prove to be a critical limitation of TOF-MRA in long-term follow-up of patients with treated intracranial aneurysms. The reason for this underestimation is likely related to the sensitivity of TOF-MRA to turbulent or slow flow, a common finding in patients after EVT.[15] Conversely, CE-MRA is substantially faster than TOF-MRA and avoids flow-related artifacts by using intravascular contrast. However, although our study showed that both DISCO-MRA and TOF-MRA had very few cases in which the MRRC was overestimated, there were a few more overestimated with DISCO-MRA (4/68) than with TOF-MRA (1/68). This finding may be explained by differences in spatial resolution and slightly larger voxel sizes of DISCO-MRA in comparison with TOF-MRA, with a potential for volume averaging.

In terms of diagnostic performance, our results are concordant with the results of prior studies, showing slightly higher performance of CE-MRA compared with TOF-MRA in identifying residual aneurysms.[16-18] However, our study reports a disproportionately lower sensitivity of TOF-MRA compared with prior reports mainly due to a high false-negative count. This finding is consistent with those of prior reports,[19-21] with the higher false-negative rate in TOF-MRA attributed to flow-related disturbance in the presence of flow-diverting stents or slow flow associated with coil embolization, despite residual/recanalized aneurysms. Our subanalysis revealed a higher proportion of aneurysm-remnant misclassification via TOF-MRA in patients treated with stents (13 versus 3 by DISCO-MRA) in comparison with 9 versus 5 in patients treated without stents.

The superior accuracy of DISCO-MRA compared with TOF-MRA, paired with its shorter acquisition time, makes it an attractive alternative for routine follow-up of endovascularly treated IAs. Shorter acquisition times can facilitate the examination of patients with claustrophobia, decrease the likelihood of a motion artifact–degraded study (Fig 4), and improve throughput. In comparison with conventional CE-MRA techniques, DISCO-MRA provides substantially faster acquisition time over a large FOV (whole-head coverage) without compromising image quality, which has traditionally been a concern with ultrafast MR imaging protocols.[22] One clear limitation of DISCO-MRA is the requirement for the administration of gadolinium-based contrast, with a small risk of an allergic reaction or other unwanted adverse effects, especially given recent concerns for tissue deposition.[23] However, the superior diagnostic performance in identifying higher class residuals may outweigh this risk. One way to mitigate the concerns about long-term and repetitive use of gadolinium injection would be to adopt a hybrid protocol of performing CE-MRA for the first 2 years, when the risk of recanalization is highest, and then switching to TOF-MRA or alternative follow-up examinations. Newer noncontrast MRA techniques have also been developed such as Silent MRA[24-26] and pointwise encoding time reduction with radial acquisition MRA,[27] with promising results in the detection of residual aneurysms.

Also, although contrast administration can increase the cost compared with non-contrast-enhanced studies (TOF-MRA) on an individual level,[6] the ultrafast protocol used allows streamlined workflow, potentially decreasing the long-term cost to an institution.

Our study has several limitations. Our sample size is relatively small. The retrospective nature introduces unknown bias. The inherent difference in spatial resolution between DISCO-MRA and TOF-MRA can limit reliable comparisons. 3D DSA was only performed in a selected group of challenging cases ($n = 17$), while 2D DSA, as a less ideal reference, was used in the remainder of

patients. The time differences (median: 99 days) between MRA examinations and DSA as the criterion standard were another limitation. It is plausible that aneurysm-occlusion grading has undergone some interval change, introducing variability in comparative analysis between DSA and MRA. However, this potential interval change in aneurysm residuals should have a modest effect in comparisons between TOF- and DISCO-MRA because they were obtained at the same time.

Another limitation is that MRRC was originally presented as a classification system for treated IAs assessed by DSA, and to the authors' knowledge, only 1 study has validated its use in MRA to date.[28] However, our study did not aim to prove the prognostic value of MRA, only to strictly prove the anatomic accuracy of DISCO-MRA compared with TOF-MRA, which aligns with the original intent of the unmodified Raymond-Roy occlusion classification to anatomically classify treated aneurysms.[29] Future studies should look at the prognostic value of the MRRC evaluated by MRA, including using the DISCO scheme in a larger sample size.

CONCLUSIONS

3T DISCO-MRA outperforms TOF-MRA with respect to accuracy and speed, with increased concordance to conventional DSA for the evaluation and grading of residual IAs after EVT. This technique may be of value in the follow-up evaluation of treated IAs.

Disclosure forms provided by the authors are available with the full text and PDF of this article at www.ajnr.org.

REFERENCES

1. Molyneux A, Kerr R, Stratton I, et al; International Subarachnoid Aneurysm Trial (ISAT) Collaborative Group. **International Subarachnoid Aneurysm Trial (ISAT) of neurosurgical clipping versus endovascular coiling in 2143 patients with ruptured intracranial aneurysms: a randomised trial.** *Lancet* 2002;360:1267–74 CrossRef Medline
2. Naggara ON, White PM, Guilbert F, et al. **Endovascular treatment of intracranial unruptured aneurysms: systematic review and meta-analysis of the literature on safety and efficacy.** *Radiology* 2010;256:887–97 CrossRef Medline
3. De Leacy RA, Fargen KM, Mascitelli JR, et al. **Wide-neck bifurcation aneurysms of the middle cerebral artery and basilar apex treated by endovascular techniques: a multicentre, core lab adjudicated study evaluating safety and durability of occlusion (BRANCH).** *J Neurointerv Surg* 2019;11:31–36 CrossRef Medline
4. Ferns SP, Sprengers ME, van Rooij WJ, et al. **Coiling of intracranial aneurysms: a systematic review on initial occlusion and reopening and retreatment rates.** *Stroke* 2009;40:e523–29 CrossRef Medline
5. Molyneux AJ, Birks J, Clarke A, et al. **The durability of endovascular coiling versus neurosurgical clipping of ruptured cerebral aneurysms: 18-year follow-up of the UK cohort of the International Subarachnoid Aneurysm Trial (ISAT).** *Lancet* 2015;385:691–97 CrossRef Medline
6. Soize S, Gawlitza M, Raoult H, et al. **Imaging follow-up of intracranial aneurysms treated by endovascular means: why, when, and how?** *Stroke* 2016;47:1407–12 CrossRef Medline
7. Korosec FR, Frayne R, Grist TM, et al. **Time-resolved contrast-enhanced 3D MR angiography.** *Magn Reson Med* 1996;36:345–51CrossRef Medline
8. Lim RP, Shapiro M, Wang EY, et al. **3D time-resolved MR angiography (MRA) of the carotid arteries with time-resolved imaging with stochastic trajectories: comparison with 3D contrast-enhanced bolus-chase MRA and 3D time-of-flight MRA.** *AJNR Am J Neuroradiol* 2008;29:1847–54 CrossRef
9. Madhuranthakam AJ, Hu HH, Barger AV, et al. **Undersampled elliptical centric view-order for improved spatial resolution in contrast-enhanced MR angiography.** *Magn Reson Med* 2006;55:50–58 CrossRef
10. Stalder AF, Schmidt M, Quick HH, et al. **Highly undersampled contrast-enhanced MRA with iterative reconstruction: integration in a clinical setting.** *Magn Reson Med* 2015;74:1652–60 CrossRef Medline
11. Griswold MA, Jakob PM, Heidemann RM, et al. **Generalized autocalibrating partially parallel acquisitions (GRAPPA).** *Magn Reson Med* 2002;47:1202–10 CrossRef Medline
12. Nael K, Drummond J, Costa AB, et al. **Differential Subsampling with Cartesian Ordering for ultrafast high-resolution MRA in the assessment of intracranial aneurysms.** *J Neuroimaging* 2020;30:40–44 CrossRef Medline
13. Mascitelli JR, Moyle H, Oermann EK, et al. **An update to the Raymond-Roy occlusion classification of intracranial aneurysms treated with coil embolization.** *J NeuroIntervent Surg* 2015;7:496–502 CrossRef Medline
14. Stapleton CJ, Torok CM, Rabinov JD, et al. **Validation of the Modified Raymond-Roy classification for intracranial aneurysms treated with coil embolization.** *J NeuroIntervent Surg* 2016;8:927–33 CrossRef Medline
15. Deutschmann HA, Augustin M, Simbrunner J, et al. **Diagnostic accuracy of 3D time-of-flight MR angiography compared with digital subtraction angiography for follow-up of coiled intracranial aneurysms: influence of aneurysm size.** *AJNR Am J Neuroradiol* 2007;28:628–34 Medline
16. Ahmed SU, Mocco J, Zhang X, et al. **MRA versus DSA for the follow-up imaging of intracranial aneurysms treated using endovascular techniques: a meta-analysis.** *J Neurointerv Surg* 2019;11:1009–14 CrossRef Medline
17. Anzalone N, Scomazzoni F, Cirillo M, et al. **Follow-up of coiled cerebral aneurysms at 3T: comparison of 3D time-of-flight MR angiography and contrast-enhanced MR angiography.** *AJNR Am J Neuroradiol* 2008;29:1530–36 CrossRef Medline
18. van Amerongen MJ, Boogaarts HD, de Vries J, et al. **MRA versus DSA for follow-up of coiled intracranial aneurysms: a meta-analysis.** *AJNR Am J Neuroradiol* 2014;35:1655–61 CrossRef Medline
19. Attali J, Benaissa A, Soize S, et al. **Follow-up of intracranial aneurysms treated by flow diverter: comparison of three-dimensional time-of-flight MR angiography (3D-TOF-MRA) and contrast-enhanced MR angiography (CE-MRA) sequences with digital subtraction angiography as the gold standard.** *J Neurointerv Surg* 2016;8:81–86 CrossRef Medline
20. Binyamin TR, Dahlin BC, Waldau B. **Comparison of 3D TOF MR angiographic accuracy in predicting Raymond grade of flow-diverted versus coiled intracranial aneurysms.** *J Clin Neurosci* 2017;42:182–85 CrossRef Medline
21. Boddu SR, Tong FC, Dehkharghani S, et al. **Contrast-enhanced time-resolved MRA for follow-up of intracranial aneurysms treated with the Pipeline embolization device.** *AJNR Am J Neuroradiol* 2014;35:2112–18 CrossRef Medline
22. Tsao J. **Ultrafast imaging: principles, pitfalls, solutions, and applications.** *J Magn Reson Imaging* 2010;32:252–66 CrossRef Medline
23. Mathur M, Jones JR, Weinreb JC. **Gadolinium deposition and nephrogenic systemic fibrosis: a radiologist's primer.** *Radiographics* 2020;40:153–62 CrossRef Medline
24. Ryu KH, Baek HJ, Moon JI, et al. **Usefulness of noncontrast-enhanced silent magnetic resonance angiography (MRA) for treated intracranial aneurysm follow-up in comparison with time-of-flight MRA.** *Neurosurgery* 2020;87:220–28 CrossRef Medline
25. Oishi H, Fujii T, Suzuki M, et al. **Usefulness of silent MR angiography for intracranial aneurysms treated with a flow-diverter device.** *AJNR Am J Neuroradiol Neuroradiol* 2019;40:808–13 CrossRef Medline
26. Takano N, Suzuki M, Irie R, et al. **Non-contrast-enhanced silent scan MR angiography of intracranial anterior circulation**

aneurysms treated with a low-profile visualized intraluminal support device. *AJNR Am J Neuroradiol* 2017;38:1610–16 CrossRef
27. Heo YJ, Jeong HW, Baek JW, et al. **Pointwise encoding time reduction with radial acquisition with subtraction-based MRA during the follow-up of stent-assisted coil embolization of anterior circulation aneurysms.** *AJNR Am J Neuroradiol Neuroradiol* 2019;40:815–19 CrossRef Medline
28. Patzig M, Forbrig R, Gruber M, et al. **The clinical value of ceMRA versus DSA for follow-up of intracranial aneurysms treated by coil embolization: an assessment of occlusion classifications and impact on treatment decisions.** *Eur Radiol* 2021;31:4104–13 CrossRef Medline
29. Raymond J, Guilbert F, Weill A, et al. **Long-term angiographic recurrences after selective endovascular treatment of aneurysms with detachable coils.** *Stroke* 2003;34:1398–403 CrossRef